Core Loss Properties of a Motor With Nanocrystalline Rotor and Stator Cores Under Inverter Excitation

Atsushi Yao[1,2], Takaya Sugimoto[1], Shunya Odawara[3], and Keisuke Fujisaki[1]

[1]Department of Advanced Science and Technology, Toyota Technological Institute, Nagoya 468-8511, Japan
[2]Department of Electrical and Computer Engineering, Toyama Prefectural University, Imizu 939-0398, Japan
[3]Department of Electrical and Electronic Engineering, Kitami Institute of Technology, Kitami 090-8507, Japan

In this paper, we develop and examine permanent magnet synchronous motors (PMSMs) by use of both stator and rotor cores made of nanocrystalline magnetic materials (NMMs). We report core loss properties of the PMSM with the NMM under inverter excitation. In addition, we compare core losses of the PMSM with conventional non-oriented (NO) steel sheets under inverter excitation to discuss the core loss characteristics of the NMM motor. In average, under inverter excitation, the reduction ratio in core loss of the PMSM made of NMM is about 60% as compared with the core loss of the PMSM with NO sheets. In particular, the average decrease obtained by using NMM rotor core instead of NO rotor core is about 30%.

***Index Terms*— Core loss, iron loss, nanocrystalline magnetic materials (NMMs), non-oriented (NO) steels, permanent magnet synchronous motor (PMSM).**

I. Introduction

THE three main types of losses in the motors correspond to the copper losses, the mechanical losses, and the core losses (iron losses). Several researchers have recently addressed the core loss reduction of the motor based on core with amorphous magnetic materials (AMMs) [1]–[12] and nanocrystalline magnetic materials (NMMs) [13], [14]. The AMM and the NMM offer core loss reduction of motor in comparison with conventional non-oriented (NO) electrical steel sheets. In particular, the NMM presents lower iron loss density in comparison with the AMM [15]. This paper aims to develop "both stator and rotor cores" with the NMM and to examine the core loss properties of the motor with nanocrystalline cores excited by a inverter.

Previous studies have shown that permanent magnet synchronous motors (PMSMs) by the use of "only stator core" with the NMM have low core losses in comparison with the NO core [13], [14]. Therefore, the next phase is to understand core loss properties of "both stator and rotor cores" with the NMM. The evaluation of both the stator and rotor cores with the NMM allows us to realize low-loss motor system.

In this paper, based on both experiments and numerical simulations, we address the core loss properties of the PMSM with the NMM stator and rotor cores under pulsewidth-modulation (PWM) inverter excitation. We compare core losses of the PMSM with the NO cores under the PWM inverter excitation to discuss the core loss characteristics of the NMM motor. In particular, we focus on core loss reduction of motor that depend on stator and rotor core materials.

Manuscript received February 22, 2018; revised May 14, 2018; accepted May 29, 2018. Date of publication June 20, 2018; date of current version October 17, 2018. Corresponding author: A. Yao (e-mail: yao@pu-toyama.ac.jp).

Color versions of one or more of the figures in this paper are available online at http://ieeexplore.ieee.org.

Digital Object Identifier 10.1109/TMAG.2018.2842431

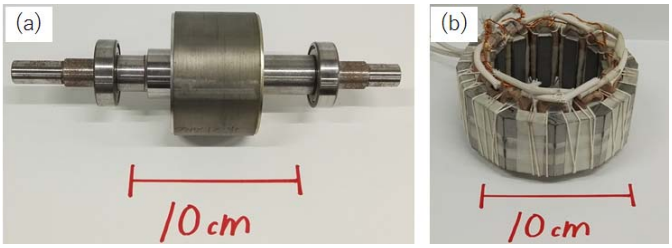

Fig. 1. Photographs of fabricated (a) rotor and (b) stator cores with NMM.

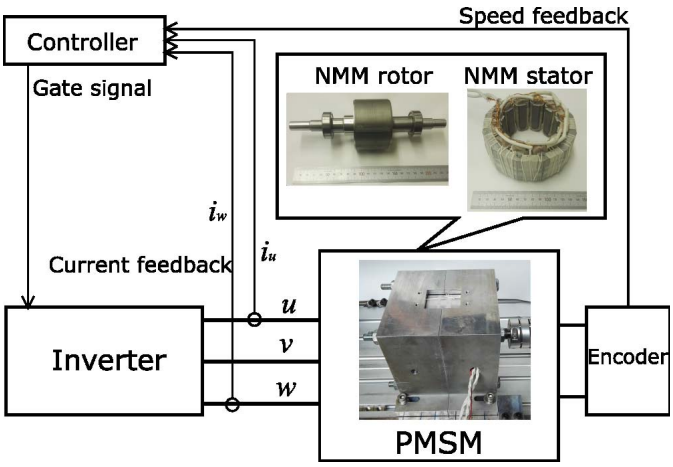

Fig. 2. Schematic of completed PMSM and control system. In this experimental system, we measure core losses under no-load condition. Here, the motor core is excited by three-phase inverter with classical PWM control.

II. Motor Core, Experimental Test Method, and Numerical Simulation Method

A. Motor Core

Fig. 1 shows the appearance of the fabricated rotor and stator cores with NMM. The fabricated rotor and stator cores are inserted into the motor casing (completed PMSM shown in Fig. 2). For comparison purposes, in this paper, the stator and rotor cores made of NO electrical steel sheets (35H300)

TABLE I
SPECIFICATIONS OF MATERIALS USED FOR MOTOR (ROTOR AND STATOR) CORES

	NO	NMM
Reference	35H300	FT-3M
Density [kg/m^3]	7650	7300
Composition	Fe-Si	Fe-Si-B-Cu-Nb
Thickness [μm]	350	18
Saturation magnetic flux density [T]	2.12	1.23
Relative permeability	1550 [16]	70000 [17]
Resistivity [$\mu\Omega$·m]	0.52 [18]	1.2 [17]

are also used. The NO electrical steel sheets and the NMM consist of Fe-Si and Fe-Si-B-Cu-Nb, respectively. Table I shows the specifications of two different materials used for the motor cores.

The nanocrystalline alloy ribbons are laminated and impregnated with acrylic resin to make the block core. The laminated block core is then cut in the shape of the rotor and stator cores using electric discharge machining. The rotor core with an outer diameter of 74-mm and a thickness of 47-mm is constructed. After that, the Sm-Fe-B bonded magnets are buried inside the rotor and then the shaft is inserted into the rotor core. The stator diameter is 128 mm and the stator core is manufactured in four separated pieces [14]. The space factor of the NMM rotor and stator cores is about 82% and 81%, respectively. The stator and rotor cores made of NO sheets reach a space factor of 99%. Here, the cores for two different materials are the same design. See [2], [12], [14] for the details of design and fabrication process of the NMM stator, NO rotor, and NO stator cores.

In this paper, we perform three kinds of motor tests. The first test, called NO-PMSM, has the stator and rotor cores made of NO sheets, the second test, called NMM-PMSM, has the stator and rotor cores made of NMM, and the third test, called NMM-NO-PMSM, has the stator core with NMM and the rotor core with NO sheets.

B. Experimental Setup of Motor Test

The total core losses of motor tests are measured under no-load condition, in which good accuracy of core loss measurement can be performed in comparison with the case in load condition. Here, the total core losses correspond to the stator, rotor and magnets losses. Fig. 2 shows the set-up of the PMSM control system, which consists of a three-phase voltage source PWM inverter with insulated gate bipolar transistors. Here, a power analyzer (PX8000, Yokogawa) is used to measure the phase voltages, the phase rms currents, and then the input active electrical power P_{in}. Conventional vector control is used for the rotational speed control. In the experiments, the core loss P_{core} is given by

$$P_{\text{core}} = P_{\text{in}} - I_{\text{motor}}^2 R - P_m \tag{1}$$

$$P_{\text{in}} = P_u + P_v + P_w \tag{2}$$

$$I_{\text{motor}}^2 = I_u^2 + I_v^2 + I_w^2 \tag{3}$$

where R (= 0.5 Ω) is the winding resistance, I_{motor} is the total rms current, $I_{u,v,w}$ are, respectively, the u, v, and w rms currents, $P_{u,v,w}$ are, respectively, the u, v, and w input powers, and P_m is the mechanical loss. In our experiments, the mechanical losses P_m are obtained by using a rotor without magnetization (see [1], [2], [12] for the details of core loss measurement and mechanical loss measurement methods). Here, the mechanical losses at 750, 1500, and 2250 r/min are 0.34, 0.88, and 1.4 W, respectively.

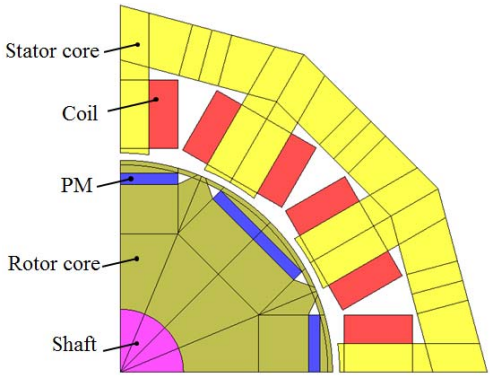

Fig. 3. Schematic of numerical model (1/4-region model). The working conditions based on the experimental results are simulated by a 2-D FEM using the JMAG software. See [2] for the details of the numerical model.

In the following experiments, the dc bus voltage V_{dc}, the d-axis current, the switching dead time, and the carrier frequency f_c are set to 250 V, 0, 3.5 μs, and 1 kHz, respectively. The motor used in this paper is the PMSM with eight poles and 12 slots. The tests are done at a rotational speed of 750, 1500, and 2250 r/min that correspond to electrical frequency f_e of 50, 100, and 150 Hz, respectively.

C. Numerical Simulation Method

Fig. 3 shows a finite-element method (FEM) model. Here, 2-D non-linear magnetic field analysis with A-method is used for our numerical simulations, which are a time-stepped simulation. By using numerical simulations, we can obtain the core loss repartition (stator, rotor, and magnets losses) and distributions.

The equation of the magnetic vector potential $\boldsymbol{A}$ is given as

$$\text{rot}(\nu \text{rot}\boldsymbol{A}) = \boldsymbol{J_0} - \sigma \frac{\partial}{\partial t}\boldsymbol{A} + \nu_0 \text{rot}\boldsymbol{M}, \tag{4}$$

where ν denotes the magnetic reluctivity, $\boldsymbol{J_0}$ is the current density in the coil parts, σ is the conductivity, ν_0 is the space reluctivity, and $\boldsymbol{M}$ (= 0.728 T) is the magnetization of the permanent magnets (PMs). Ideal phase voltage waveforms based on the experimental results are used as the input of the numerical analysis.

In our simulations, the magnet losses W_{mag} are calculated based on the analyzed eddy current density and the electrical conductivity. Here, the measured electrical conductivity σ of the PM is 2344 S/m. In our simulations, the eddy currents in the stator and rotor parts are not calculated and then the stator core losses W_{stator} and rotor core losses W_{rotor} (soft magnetic core losses) are calculated from Steinmetz equation. Therefore, in numerical simulations, the entire core losses W_{nuloss} are

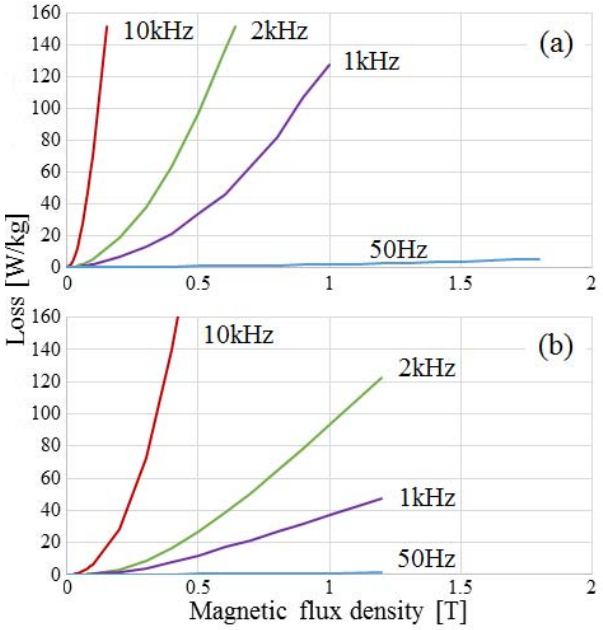

Fig. 4. Representative loss characteristics as a function of magnetic flux density at 50 Hz, 1 kHz, 2 kHz, and 10 kHz. In our numerical simulations, loss characteristics at 50 Hz, 400 Hz, 1 kHz, 2 kHz, 5 kHz, and 10 kHz are used as the input to obtain the core losses. (a) NO. (b) NMM.

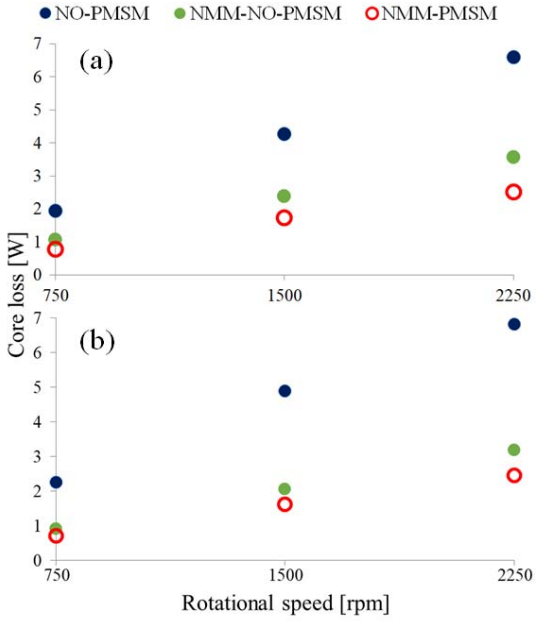

Fig. 5. (a) Experimentally entire core losses as a function of rotational speed. For NO-, NMM-NO-, and NMM-PMSM, the core losses are measured under no-load condition. (b) Corresponding numerical entire core losses calculated by JMAG software.

given by

$$W_{\text{nuloss}} = W_{\text{mag}} + W_{\text{stator}} + W_{\text{rotor}} \tag{5}$$

$$W_{\text{stator}} + W_{\text{rotor}} = \sum_{\text{ie}=1}^{ne}\left[\sum_{k=1}^{N}\{\alpha(|B_k|)f_k\}\right]\upsilon_{\text{ie}} + \sum_{ie=1}^{ne}\left[\sum_{k=1}^{N}\beta(|B_k|, f_k)f_k^2\right]\upsilon_{\text{ie}} \tag{6}$$

$$W_{\text{mag}} = \frac{1}{T}\sum_{t=1}^{\text{step}}\sum_{ie=1}^{\text{ne}}\frac{J(t)_{\text{ie}}^2}{\sigma_{\text{ie}}}\upsilon_{\text{ie}}\Delta t \tag{7}$$

where α denotes the coefficient of hysteresis loss, β is the coefficient of eddy current loss, T is the fundamental period, υ is the volume obtained by multiplying the element area by the core length, B is the magnetic flux density, f is the frequency, J is the eddy current density, ie is the element number, and k is the harmonic order. α and β are calculated based on loss characteristics of the materials (NO sheets and NMM) as shown in Fig. 4. In this paper, we consider not the loss related to the material itself but the core loss caused by factors, such as the core geometrical configuration and so on, in the PMSM by numerical simulations. Therefore, we use the fitting loss characteristics shown in Fig. 4.

The numerical simulation method is summarized as follows. First, the iron loss characteristics of the NO and the NMM are obtained from catalog data [16] and loss in a ring specimen, respectively. Second, we fit the loss characteristics of NO sheets and the NMM to equalize the numerical data [each numerical core loss of the NO-PMSM and the NMM-PMSM at 2250 r/min shown in Fig. 5(b)] to the experimental data [each experimental core loss of the NO-PMSM and the NMM-PMSM at 2250 r/min shown in Fig. 5(a)]. and Finally, based on the fitting loss characteristics at 2250 r/min, we calculate the core losses of the NO-, and the NMM-PMSM at 750 and 1500 r/min, respectively. In addition, we also calculate the core losses of the NMM-NO-PMSM at 750, 1500, and 2250 r/min. See [2], [12] for more details of numerical simulation model and methods.

III. Results and Discussion

Fig. 5(a) shows experimental results of entire core losses as a function of the rotational speed under no-load condition. Here, the NO-, NMM-NO-, and NMM-PMSM under the PWM inverter excitation are evaluated. The core loss increases with increasing the rotational speed for each motor test. The NO-PMSM (NMM-PMSM) exhibits core losses of about 2.0, 4.3, and 6.6 W (0.8, 1.7, and 2.5 W) at 750, 1500, and 2250 r/min, respectively. The core loss of the NMM-NO-PMSM is about 1.1, 2.4, and 3.6 W at 750, 1500, and 2250 r/min, respectively. In average, under PWM inverter excitation, the reduction ratio in core loss of the NMM-PMSM (NMM-NO-PMSM) is about 60% (45%) as compared with the core loss of the NO-PMSM. These results show that the core loss reduction depends not only on the stator core but also on the rotor core. In particular, the average decrease obtained by using the NMM rotor core instead of the NO rotor core is about 30%.

Here, the current values of the NMM-PMSM are 0.33, 0.63, and 0.99 A at 750, 1500, and 2250 r/min, respectively. Fig. 5(a) shows the core losses under different current density. The NMM-PMSM (NO-PMSM) exhibits copper losses of about 0.16 W (0.11 W) at 750 r/min, of about 0.60 W (0.39 W) at 1500 r/min, and of about 1.5 W (0.96 W) at 2250 r/min, respectively. The copper losses of the NMM-NO-PMSM are

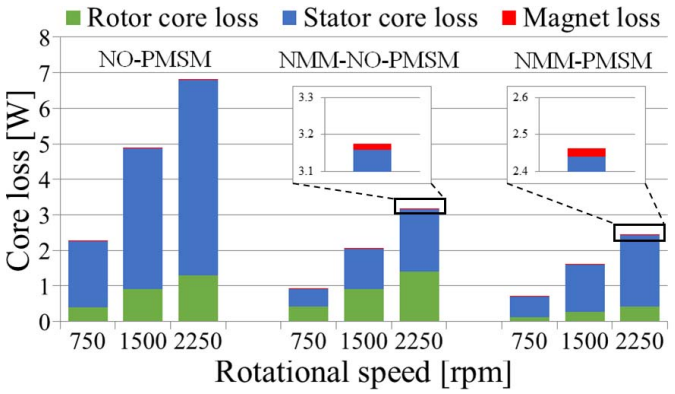

Fig. 6. Numerical core loss repartition for NO- (left), NMM-NO- (center), and NMM-PMSM (right). These results are calculated by using Eqs. (6) and (7). Inset: magnified figures of W_{mag} at 2250 r/min.

0.10 W at 750 r/min, 0.39 W at 1500 r/min, and 0.97 W at 2250 r/min, respectively. Here, the mechanical loss of the NO-, NMM-NO-, and NMM-PMSM at 750 r/min accounts for 14, 22, and 26% of the input power, respectively. The percentage of the mechanical loss to the input power in the NMM-PMSM is higher than that in the NO- and NMM-NO-PMSM.

Fig. 5(b) shows the entire core losses as a function of the rotational speed simulated by JMAG software. The experimental core losses [Fig. 5(a)] are consistent with the calculated core losses [Fig. 5(b)]. Here, in the NMM-NO-PMSM, there is the slight difference between experimental and numerical results. This is mainly due to the fact that the slight difference between the stator and rotor cores for a deterioration of the core losses caused by the manufacture process are not taken into account in the numerical simulations. In our future work, we will evaluate the building factor, which can understand the core losses caused by factors, such as the manufacturing process and so on [19], [20], in each core (stator and rotor cores).

Fig. 6 shows core loss repartition between the rotor, stator, and magnets for the NO-, NMM-NO-, and NMM-PMSM. In average, the W_{mag} of the NO-, NMM-NO-, and NMM-PMSM accounts for less than 1% of the total core losses, because the Sm-Fe-B bonded magnets exhibit low loss. Therefore, almost all losses for the entire core losses correspond to losses derived from soft magnetic materials (NO and NMM). In the NMM-PMSM (NMM-NO-PMSM), the interlinkage magnetic flux Φ of copper coil induced by the PM is 27.6 (25.2) mWb at 1500 r/min. The NMM-PMSM shows slightly large interlinkage magnetic flux Φ compared with that of the NMM-NO-PMSM. Therefore, because of slightly large Φ, the stator core losses W_{stator} of the NMM-PMSM are slightly larger than those of the NMM-NO-PMSM. The details of the relationship between the rotor core materials and the interlinkage magnetic flux will be investigated.

Fig. 7 shows the core loss distributions of the NO-, NMM-NO-, and NMM-PMSM for the rotational speed of 1500 r/min. The core loss density in the NMM stator and rotor cores is significantly lower than that in stator and rotor cores with NO sheets. These results confirm the benefit of using not only the NMM stator core but also the NMM rotor core to reduce the core losses of the motor.

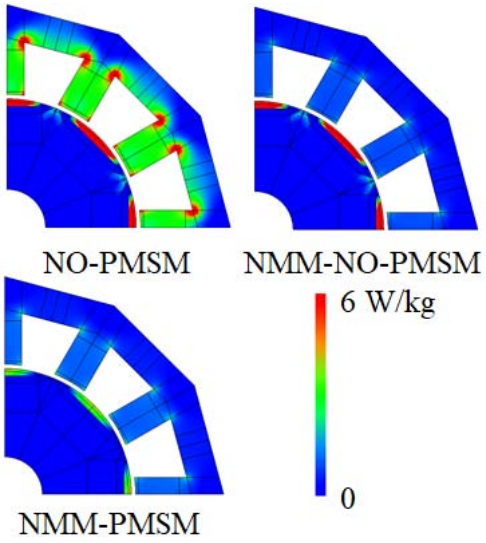

Fig. 7. Numerical core loss distributions at 1500 r/min for NO-, NMM-NO-, and NMM-PMSM.

IV. Conclusion

We for the first time developed and examined the PMSM by use of "both stator and rotor cores" made of the NMM. In average, under the PWM inverter excitation, the reduction ratio in core loss of the NMM-PMSM (NMM-NO-PMSM) was about 60% (45%) as compared with the core loss of the NO-PMSM. In particular, the average decrease obtained by using the NMM rotor core instead of the NO rotor core was about 30%. These results open the way to further research for ultimate low-loss motor system based on both the rotor and stator core with the NMM. In our future works, we will evaluate the torque capacity as well as the decrease of core losses under load condition. The efficiency comparison between the NO-, NMM-NO-, and NMM-PMSM under load condition will also be investigated.

Acknowledgment

This work was supported in part by the Ministry of Education, Culture, Sports, Science and Technology Program, Japan, for private universities and in part by the New Energy and Industrial Technology Development Organization.

References

[1] N. Denis, Y. Kato, M. Ieki, and K. Fujisaki, "Core losses of an inverter-fed permanent magnet synchronous motor with an amorphous stator core under no-load," *AIP Adv.*, vol. 6, p. 055916, Mar. 2016.

[2] S. Okamoto, N. Denis, Y. Kato, M. Ieki, and K. Fujisaki, "Core loss reduction of an interior permanent-magnet synchronous motor using amorphous stator core," *IEEE Trans. Ind. Appl.*, vol. 52, no. 3, pp. 2261–2268, May/Jun. 2016.

[3] M. Dems and K. Komeza, "Performance characteristics of a high-speed energy-saving induction motor with an amorphous stator core," *IEEE Trans. Ind. Electron.*, vol. 61, no. 6, pp. 3046–3055, Jun. 2014.

[4] A. Chiba *et al.*, "Test results of an SRM made from a layered block of heat-treated amorphous alloys," *IEEE Trans. Ind. Appl.*, vol. 44, no. 3, pp. 699–706, May 2008.

[5] Z. Wang, Y. Enomoto, R. Masaki, K. Souma, H. Itabashi, and S. Tanigawa, "Development of a high speed motor using amorphous metal cores," in *Proc. IEEE 8th Int. Conf. Power Electron. ECCE Asia (ICPE & ECCE)*, May/Jun. 2011, pp. 1940–1945.

[6] G. S. Liew, W. L. Soong, N. Ertugrul, and J. Gayler, "Analysis and performance investigation of an axial-field PM motor utilising cut amorphous magnetic material," in *Proc. IEEE 20th Australas. Universities Power Eng. Conf. (AUPEC)*, Dec. 2010, pp. 1–6.

[7] Z. Wang *et al.*, "Development of a permanent magnet motor utilizing amorphous wound cores," *IEEE Trans. Magn.*, vol. 46, no. 2, pp. 570–573, Feb. 2010.

[8] Z. Wang *et al.*, "Development of an axial gap motor with amorphous metal cores," *IEEE Trans. Ind. Appl.*, vol. 47, no. 3, pp. 1293–1299, May/Jun. 2011.

[9] Y. Enomoto *et al.*, "Evaluation of experimental permanent-magnet brushless motor utilizing new magnetic material for stator core teeth," *IEEE Trans. Magn.*, vol. 41, no. 11, pp. 4304–4308, Nov. 2005.

[10] T. Fan, Q. Li, and X. Wen, "Development of a high power density motor made of amorphous alloy cores," *IEEE Trans. Ind. Electron.*, vol. 61, no. 9, pp. 4510–4518, Sep. 2014.

[11] R. Kolano, K. Krykowski, A. Kolano-Burian, M. Polak, J. Szynowski, and P. Zackiewicz, "Amorphous soft magnetic materials for the stator of a novel high-speed PMBLDC motor," *IEEE Trans. Magn.*, vol. 49, no. 4, pp. 1367–1371, Apr. 2013.

[12] A. Yao, T. Sugimoto, S. Odawara, and K. Fujisaki, "Core losses of a permanent magnet synchronous motor with an amorphous stator core under inverter and sinusoidal excitations," *AIP Adv.*, vol. 8, no. 5, p. 056804, 2018.

[13] N. Nishiyama, K. Tanimoto, and A. Makino, "Outstanding efficiency in energy conversion for electric motors constructed by nanocrystalline soft magnetic alloy 'NANOMET' cores," *AIP Adv.*, vol. 6, no. 5, p. 055925, 2016.

[14] N. Denis, M. Inoue, K. Fujisaki, H. Itabashi, and T. Yano, "Iron loss reduction in permanent magnet synchronous motor by using stator core made of nanocrystalline magnetic material," *IEEE Trans. Magn.*, vol. 53, no. 11, Nov. 2017, Art. no. 8110006.

[15] H. Kosai, Z. Turgut, T. Bixel, and J. Scofield, "Performance comparison of finemet and metglas tape cores under non-sinusoidal waveforms with dc bias," *IEEE Trans. Magn.*, vol. 52, no. 7, Jul. 2016, Art. no. 8400704.

[16] *Non-Oriented Electrical Steel Sheets*, (in Japanese), Nippon Steel Corp., Tokyo, Japan, 2004.

[17] *Nanocrystalline Soft Magnetic Materials*, (in Japanese), Hitachi Met. Ltd., Tokyo, Japan, 2016. [Online]. Available: http://www.hitachi-metals.co.jp/products/elec/tel/pdf/hl-fm9-h.pdf

[18] *Non-Oriented Electrical Steel Sheets*, (in Japanese), Nippon Steel and Sumitomo Metal Corp., Tokyo, Japan, 2015. [Online]. Available: https://www.nssmc.com/product/catalog_download/pdf/D005je.pdf

[19] A. Yao *et al.*, "PWM inverter-excited iron loss characteristics of a reactor core," *AIP Adv.*, vol. 7, no. 5, p. 056618, 2017.

[20] A. Yao, A. Adachi, and K. Fujisaki, "Iron loss characteristics of electric motor in high-temperature environment," in *Proc. IEEE Int. Electr. Mach. Drives Conf. (IEMDC)*, May 2017, pp. 1–7.